INVESTMENT CASTING OF ALUMINIUM ALLOY A356 USING PRIMECAST® AND PMMA ADDITIVE MANUFACTURING MATERIALS FOR SACRIFICIAL PATTERNS

N.P. Nkhasi[1*], W.B. du Preez[2] and J.G. van der Walt[3]

ABSTRACT

Investment casting is a manufacturing process that uses sacrificial patterns and ceramic shells to produce a cast part. Castings produced from this process have smooth surfaces and an excellent dimensional accuracy. The process involves pattern making, mould making, burnout and casting. In this study, aluminium alloy A356 castings were produced from patterns manufactured using two additive manufacturing technologies and materials, namely PrimCast® and PMMA. Metrology was performed on all the castings through Micro-CT scanning and comparison of different features of the castings from the two types of patterns was done. Dimensional accuracy of the two pattern making approaches are discussed.

[1, 2, 3] Department of Mechanical Engineering
Central University of Technology, Free State, South Africa
[1]nthatengnp@gmail.com [2]wdupreez@cut.ac.za [3]jgvdwalt@cut.ac.za

1. INTRODUCTION

1.1 Investment casting

The investment casting process, dates back over 5 000 years to artists and sculptors of ancient Egypt and China [1]. The typical process consists of pattern making, investing (dipping and stuccoing), dewaxing and firing, casting, knock-out, cut-off and, testing and inspection. The term investment casting has been derived from the typical use of mobile slurry to form a hard shell. In this process a sacrificial pattern is coated with refractory ceramic slurry that can set at room temperature to produce a shell mould (or block mould). In order to obtain a good surface finish on the casting, the quality of the coating is important. The coating thickness should also be uniform across all features of the pattern to ensure even heat transfer properties during the casting process. A pattern is needed for every casting to be produced. Cast parts are formed by melting out (or dissolution) of the sacrificial pattern and pouring the molten metal into the mould cavity. After the metal has solidified within the ceramic mould, the ceramic shell is broken away and the casting taken out [2]. Wax was conventionally used to make sacrificial patterns, but in recent times it was found that patterns produced from Additive Manufacturing (AM) technology can also be used, especially during the development stage of new products or in small volume production [3].

1.2 Rapid investment casting

The use of AM sacrificial patterns for investment casting can be referred to as Rapid Investment Casting (RIC). AM sacrificial patterns were first used in 1989 [4]. In RIC the pattern is designed using Computer Aided Design (CAD) software and is then manufactured using an AM machine. Depending on the AM technology used, gates and vents are attached to the pattern. The vents are used to allow steam to enter the pattern during autoclaving and to allow airflow through the mould during burnout replacing oxygen used in combustion [5]. The assembly is then repeatedly dipped in ceramic slurry. The pattern is then melted or burnt out, leaving a cavity in the shape of the part to be cast. A metal alloy is melted, often in an induction furnace, and poured into the preheated shell. After cooling the shell is broken away and the gates and vents are ground off [6]. In RIC a key consideration is pattern modification to prevent shell cracking and minimize residual ash. Ceramic shells have a very low coefficient of thermal expansion, so any expansion of the pattern during the burnout cycle may cause the shell to crack [7]. During the burnout process, the pattern will combust and release some gas. The vents allow the gas to escape during burnout and promote air flow for combustion [8]. Since AM patterns expand more than the traditionally used wax, additional layers of the ceramic slurry are required to minimize shell cracking during the burnout process [9].

The key advantage of RIC is that it eliminates the need for wax tooling for low-volume production typical in prototyping, pre-series, customised or specialised component productions. Injection moulds for wax patterns are expensive and the building of the tool can take four to six weeks. Through using RIC patterns the tooling cost is eliminated and the lead time for a cast part is reduced to just 10 days on average. The ensuing mould preparation and casting process is the same irrespective of how the pattern was produced, be it using conventional wax techniques or RIC technology [10].

From the literature it was found that little research has been done. Initial work done by Dimitrov et al. [4] on rapid pattern making in investment casting of a light metal was found. In their study the comparison between patterns produced from three additive manufacturing technologies namely 3D printing, selective laser sintering and thermojet was done using a coordinate measuring machine (CMM). From the results found with aluminium casting after evaluating the descriptive statistics, features measured and the dimensional accuracy indexed, it was concluded that the selective laser sintering pattern produced the best casting in terms of dimensional accuracy.

A recent article from Tom Mueller [12] compares the patterns and castings from four AM technologies, namely stereolithography (QuickCast™), laser sintering (QuickForm™), Projet printing (Projet Wax™), and binder jetting (PMMA). In the first part of the article he compares the performance of the printers, the second part compares the operating costs and in the last part the four leading methods of creating printed patterns for investment castings are compared. The analysis was based on the author's experience and it was concluded that there was no single 'best' pattern printing technology. For each of the four technologies, applications existed for which they were the best alternative. Clearly, requirements for investment castings vary considerably depending on the application of the casting.

It was also found that there has been significant work done on PMMA [11, 12, 13, 14] and PrimeCast® [4, 8, 9, 15] trying to show that they can replace the lost wax process in investment casting. However, no research was found on direct comparison between the two AM materials for use as sacrificial patterns for investment casting.

1.3 Previous work

In previous work by Nkhasi et al. [16], sacrificial pattern geometry for investment casting that could be built with PrimeCast® and Poly(Methyl Methacrylate) (PMMA) was selected. Comparisons were performed on patterns built in PrimeCast® and PMMA respectively, which were produced using AM technology. The patterns were replicas of the casting to be produced and they did not include allowances for the expansion and contraction which occur during the casting process. The investment casting patterns built in PrimeCast® were manufactured through laser sintering on an EOSINT P380 AM machine at Central University of Technology (CUT). Those that were built in PMMA were manufactured at Vaal University of Technology (VUT) using Voxeljet 3D printing technology, which is a binder jetting process. The patterns included features such as thin walls, cavities, different surface textures and angles that are challenging to produce using the mentioned AM technologies and the investment casting process. Metrology using micro computed tomography (micro-CT) scanning was performed on each of the produced patterns and results were reported. It was found that both technologies were able to produce the required part but it was also clear that they did not show the same accuracy. This paper is now reporting on the preparation of ceramic moulds (shell making, pattern extraction and firing), characterizing of the quality of the moulds, casting of the metal alloy into the moulds and metrology on the castings. A comparison of the moulds and different features of the castings from the two types of patterns is reported.

The focus of this study is more on the difference in dimensional accuracy of the two technologies. The manufacturing lead times for the two patterns were not considered in this study because both manufacturing process are automated and the patterns can be built overnight. Furthermore, there is no discussion on the comparison of the cost associated with the manufacturing of the two AM patterns, but relevant information on where the two patterns were manufactured is shared.

2. METHODOLOGY

2.1 Mould making process

For research performed for this study, mould making and casting were done at Council for Scientific and Industrial Research (CSIR). The patterns were prepared by attaching gates and vents to the AM patterns. Ten vents were attached to the PrimeCast® pattern while no vents were used with the PMMA pattern as shown in Figure 1. The gating and vents were produced by wax injection using suitable dies at the CSIR. The assemblies were then cleaned using wax pattern cleaner and de-ionized water to remove any debris and carbon from the wax. The assemblies were then left to dry in air.

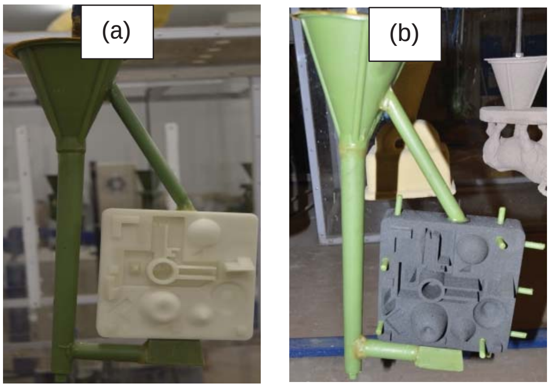

Figure 1: Sacrificial patterns with gating and vents: PMMA (a) and PrimeCast® (b).

Once the assemblies were dry, they were dipped into the primary or face coat. The primary slurry consisted of inoculated cobalt aluminate. The assemblies were dipped into the slurry very slowly and carefully to make sure that no air was entrapped while dipping. When the assemblies were taken out of the slurry it was ensured that no bubbles were trapped on the assemblies and, if present, they were removed since this could affect the casting, this coat allows for the reproduction of fine detailed features. The dipping was followed by stuccoing with fine alumina sand and the assemblies were left to dry. The dipping and stuccoing were repeated four times, with subsequent drying for four hours. Lastly, they were dipped in the backup coat (fibre reinforced fused silica) and stuccoed with fine fused silica sand after the first dipping and then coarser silica sand after the last dipping. The assemblies were left to dry for 24 hours at 22 ^{0}C. The flow diagram in Figure 2 below illustrates the process.

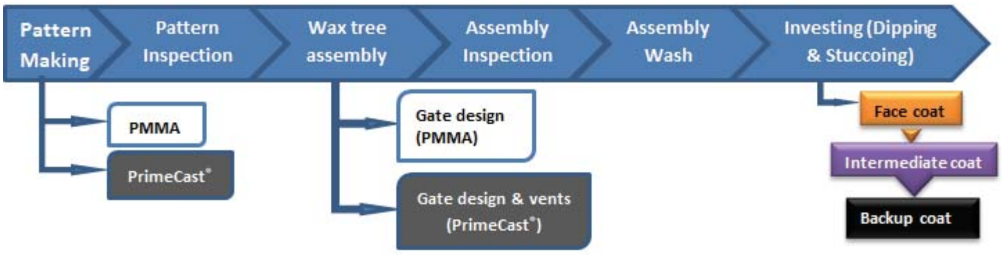

Figure 2: The flow diagram of mould making.

2.2 Burnout Processes

2.2.1 Burnout Procedure for PMMA patterns

PMMA patterns were burned out in an autoclave, with the wax used for gates melting out first, leaving an opening for the patterns to flow through. The remaining amount of pattern was burned out in a furnace.

2.2.2 Burnout Procedure for PrimeCast® patterns

In the first attempt, the patterns were removed in the autoclave using the same setting as the PMMA patterns. However, shell cracking occurred during the autoclaving of the PrimeCast® pattern, so it was realised that a redesign was needed of the PrimeCast® pattern. Electro Optical Systems (EOS), the supplier of the PrimeCast®, was consulted on how to go about the redesign and burn-out procedure of the PrimeCast® pattern for suitability as sacrificial pattern for investment casting. The redesign included manufacturing the pattern with a low laser power setting and a special burnout process. The process included two stages: autoclaving and burn-out process. The vents were opened prior to autoclaving; the wax that was used for gates and vents was melted out completely at around 150 ^{0}C using a boiler clave at the CSIR. The surface of the PrimeCast® pattern started to melt but could not flow out at this temperature. The pressure was then increased to 5 Bar and the temperature to around 200 ^{0}C for 2 hours. Most of the pattern material started to flow out, leaving some residue on the shell walls as shown in Figure 3(a). During autoclaving the pattern could flow out of the shell as quick as possible through the vents. The shells were then taken to a furnace for burn-out and the temperature was gradually increased until it reached 650 ^{0}C as shown in Figure 4. At this temperature the shells were white; this was an indication that all the PrimeCast® material had burned out completely as shown in Figure 3(b).

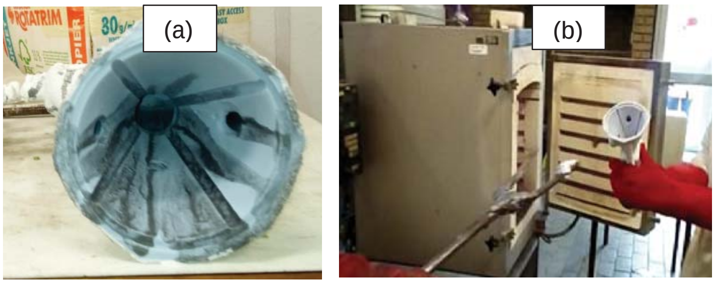

Figure 3: Shell with pattern residue (a) and White clean shell from the furnace (b).

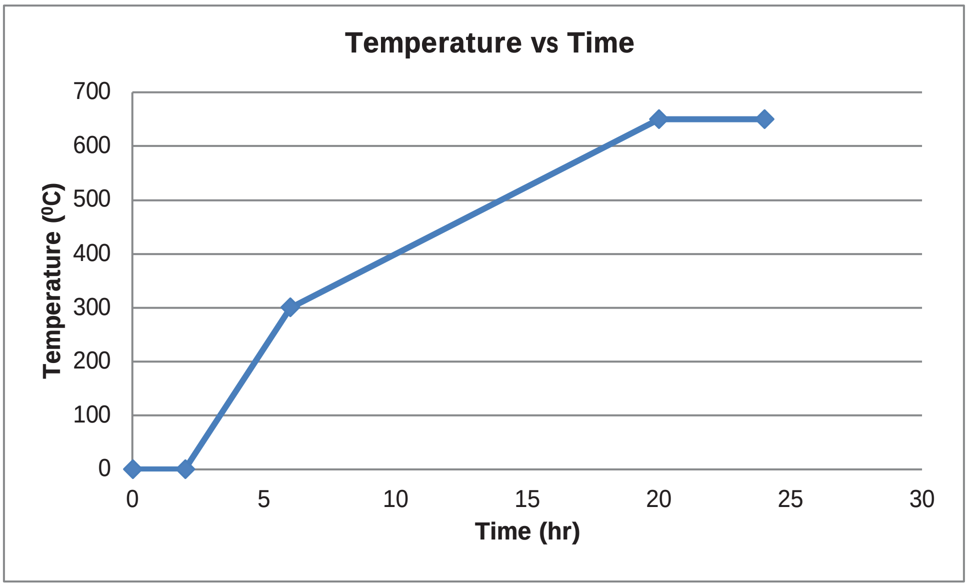

Figure 4: Temperature profile used for the burn-out furnace.

2.3 Casting Process

When the entire pattern residue had been removed from the shell, the shells were cooled and the vent holes patched using high temperature glue. The shells were then preheated to 600 ^{0}C just before pouring molten metal into them. The clay graphite crucible used with the furnace was pre-heated empty in order to minimise the temperature gradient across its wall. The crucible was preheated slowly to 200 ^{0}C for 2 hours, to eliminate any moisture, and then gradually raised to 1100 ^{0}C on full power to achieve a uniform bright red condition over the whole crucible. The temperature was then dropped to 700 ^{0}C over 8 hours before the crucible was fed with aluminium ingots. It was important that the crucible body temperature was equivalent to or slightly above that of the molten metal in order to minimise thermal stress. The aluminium ingots were cleaned before they were placed into the crucible to avoid contamination of the molten metal or flame due to impurities. They were loaded into the crucible very loosely at the time until the required quantity had been melted so as to avoid the ingots expanding and cracking the crucible. The temperature of the molten metal was recorded just before it was poured into the shell cavity as show in Figure 15 below.

Figure 5: The furnace and the recorded temperature during melting of aluminium alloy.

The liquidus temperature of aluminium A356 is 615 ^{0}C, therefore, the temperature of 670 ^{0}C was recorded as the pouring temperature for the molten metal. The oxide layer was removed prior to pouring. During the pouring the hot shells were removed one by one from the furnace and then filled with molten metal as shown in Figure 6. The filling was done carefully so that no air was trapped during filling. After the shells were filled with molten metal, they were left to cool in air. The final step was to clean-up the castings by removing the shells and grinding off the gates and vents.

Figure 6: Pouring of the molten metal into the shell (a) and the shell with molten metal left to cool in air. .(b)

2.4 Metrology Process

Four castings, two produced from PrimeCast® patterns and two from PMMA patterns, were scanned at Stellenbosch University (SU) using a micro-CT scanner [17]. The castings produced from PrimeCast® patterns were labelled PC1 and PC2, while those from PMMA patterns were labelled PMMA1 and PMMA2. A General Electric Phoenix V|Tome|X L240 / NF180 machine was used for scanning. X-ray settings used were 200 kV and 200 µA. The machine acquires 3000 images in a full rotation with an image acquisition time of 600 ms per image.

The micro-CT scanner settings were the same for all the samples scanned and are illustrated in Table 1 below. Detector shift was activated to minimize ring artefacts. The sample was positioned on the scanner's rotating stand at such an angle so that no feature on the sample was parallel to the X-ray beam as it rotated. The sample was also fixed to the table to ensure that it would not move during scanning as shown in Figure 7. Background calibration was performed and the scan time was approximately 30 minutes per scan. Reconstruction of the sample was done with system-supplied Datos reconstruction software. Analysis was performed with Volume Graphics VGStudio Max 3.2 Voxel data analysis and visualization.

Table 1: Micro-CT scanner settings.

Geometry		Detector		X-ray	
Voxel size	125 µm	Average	1	Voltage	200 kV
Magnification	1.6	Skip	0	Current	200 µA

Figure 7: Sample positioned on the scanner's rotating stand.

3. RESULTS AND DISCUSSIONS

Micro-CT scanners provide very accurate dimensions of scanned parts. Measurements were performed by comparing the CT model of a casting with the CAD model. The data includes both internal and external surface information. For the comparison to be done, the two models needed to be aligned and the alignment tool used was an automatic best fit. Once the two models were aligned, a simple 3D comparison option automatically creates a coloured view showing all the dimensional differences between the two models. Tolerance values were from -1.5 mm to 1.5 mm for all the comparisons done. All the dimensional differences between the CAD models and the CT surfaces are represented by colours. Tolerances indicating best fit are shown in green. Yellow denotes the areas where the CT scan measurements are larger than the original CAD model and blue indicates measurements smaller than the CAD model.

Each feature on the benchmark part had its own dimensional accuracy parameter to be measured, and the purpose for each feature is outlined in Table 2 below.

Table 2: Features on the benchmark part and their purposes.

Feature	*Purpose*
Cubes	Straightness, repeatability, linear accuracy
Rectangular Protrusion	Perpendicularity, linear accuracy
Pyramid	Angularity, accuracy
Sphere (half)	Symmetry, repeatability of a constantly changing sloping profile, axial runout, radial runout
Cone	Constant sloping profile, taper, axial runout, radial runout, symmetry
Free-form (conical)	Non-constant sloping profile axial runout, radial runout, symmetry
Free-form (sinkhole)	Non-constant sloping profile axial runout, radial runout, symmetry
Wedges	Angularity
Rectangular Hole	Perpendicularity
Cylindrical Hole/ Hollow Cylinder	Concentricity, circularity, accuracy
Triangular Hole	Angularity, perpendicularity
Flat thin walls	Parallelism, thickness
Square base	Flatness, straightness, parallelism
Mechanical features	Competence of machine to build particular features (visual inspection)
Yes/No Features	Machine's ability to build certain features (visual inspection)

Figure 8 shows the geometrical results obtained from the top and bottom of a casting as compared to the associated PMMA pattern and its deviation distribution from that PMMA sacrificial pattern. There are noticeable round smooth walled cavities and irregular shaped mass on the bottom of the casting. Blue and red are visible on the surface of the features where the symmetry was tested; features like half sphere, freeform (conical and sinkhole) and cone. The sharp corners and the fillet are well presented in green. Flat surfaces of the casting are also green showing the best fit, except the flat surface of the rectangular protrusion where there is blue toward the long corner edge. Angular surfaces of wedges and the small triangular hole show accurate results. The blue and red are also noticeable on the inside and outside of the square base respectively. The hollow cylinder was also green with just small defects; this feature was used to test concentricity and circularity. The pyramid was covered in green as well as the rectangular hole. The two cubes and two half cubes were used to test for repeatability and they were situated towards the margin of the casting. Both cubes and both half cubes have almost the same colours, green is predominate on the top flat surfaces with traces of red on the vertical surfaces. The shape of the deviation distribution is skewed to the right, while the peak of the distribution peak is slightly off centre toward the left (-0.2 mm) and the tail stretches to the right. From the deviation distribution, green is spread from -0.7 mm to 0.7 mm showing the highest fraction (about 85%) of the total area of the casting. About 11% of the area is found in the range from -1.5 mm to -0.7 mm, denoted in blue. The remaining area, denoted by red, which is about 4%, is found in the range 0.7 mm to 1.5 mm.

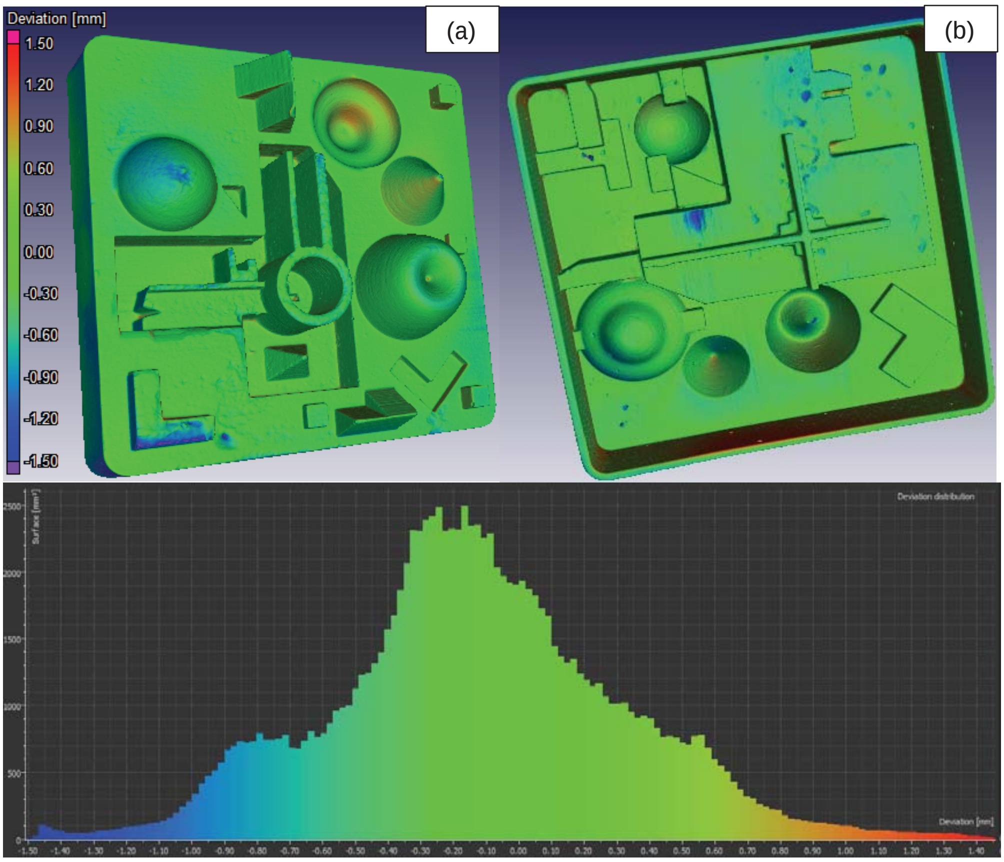

Figure 8: Casting results of the top (a), bottom (b) and the deviation distribution results from the PMMA pattern (graph below (a) and (b)).

The geometrical results for a casting from a PrimeCast® pattern showed only casting defects that could be associated with bubbles that might have been entrapped in the pattern wall by the primary slurry during mould making. They appear as small, smooth spherical or oval shaped excess metal on the casting on the corners and edges of some features. From Figure 9, it can be seen that red and blue are mostly seen on the features with repeatability of a constantly changing sloping profile (cone and sphere), non-constant sloping profile, axial runout (freeform (conical and sinkhole)), and on the inside and outside of the square base. The flat surface of almost every feature is green. The surfaces of the features that are perpendicular to the top surface of the part are blue and red. The hollow cylinder as well as the flat thin walls is green. The green on the sharp corners and the fillets indicate that they were exact replicas of the pattern. Blue is mostly seen of the surfaces of the features that are facing towards the margin of the casting, features such as half sphere and rectangular protrusion on top view of the casting. The surrounding walls are predominately blue outside and red inside. The hollow rectangle as well as the rectangular hole are green with drops of red.

The shape of the deviation distribution complies with a normal distribution, except that it has a large peak at the tail that stretches to the left. In the range -0.7 mm to 0.7 mm represented in green, the highest fraction of the total area, namely 68% is found. The range -1.5 mm to -0.7 mm is displayed in blue and represents about 20% of the total area, while the remaining area (about 12%) is red.

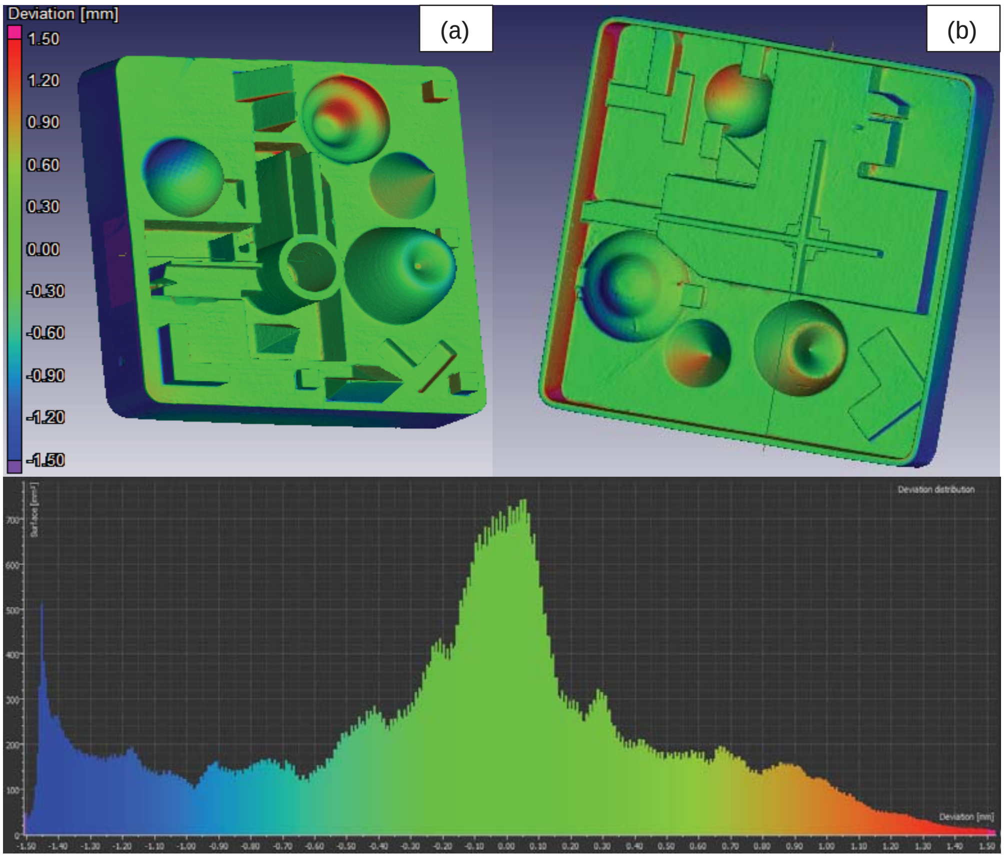

Figure 9: Casting results of the top (a), bottom (b) and the deviation distribution results from the PrimeCast® pattern (graph below (a) and (b)).

An analysis was done on five selected features from each casting, which were cube, rectangular protrusion, cone, freeform (conical) and freeform (sinkhole), as well as for the full volume of a casting. The analysis results for these features are tabulated in Table 3, which also gives the minimum and maximum deviation, the mean and the standard deviation.

Table 3: Analysis from five selected feature of the castings.

Full Volume				
Castings	***Left (mm)***	***Right (mm)***	***Mean (mm)***	***Deviation (mm)***
PMMA1	-1.50	1.50	-0.14	0.45
PMMA2	-1.50	1.50	-0.11	0.40
PC1	-1.50	1.50	-0.14	0.65
PC2	-1.50	1.50	-0.11	0.67
Cube				
PMMA1	-0.75	0.53	-0.15	0.45
PMMA2	-0.63	0.45	-0.11	0.34
PC1	-1.62	1.29	-0.01	0.98
PC2	-1.77	1.54	-0.02	1.12
Rectangular protrusion				
PMMA1	-1.76	1.63	-0.63	0.69
PMMA2	-0.78	1.47	-0.21	0.46
PC1	-1.46	1.44	-0.13	0.71
PC2	-1.46	1.38	-0.15	0.65
Cone				
PMMA1	-1.39	1.21	0.02	0.41
PMMA2	-1.04	1.50	0.04	0.29
PC1	-1.20	1.30	-0.12	0.64
PC2	-1.48	1.98	-0.07	0.79
Freeform (conical)				
PMMA1	-1.49	1.03	-0.15	0.34
PMMA2	-1.48	0.98	-0.04	0.25
PC1	-1.01	1.14	-0.15	0.47
PC2	-1.47	1.22	-0.11	0.52
Freeform (sinkhole)				

PMMA1	-1.44	0.98	-0.04	0.40
PMMA2	-0.87	0.75	-0.08	0.33
PC1	-1.51	1.46	-0.12	0.66
PC2	-1.49	1.64	-0.01	0.71

When the tolerances were set at -1.5 mm to 1.5 mm for full volume, the surface area within this range of PMMA1 and PMMA2 was 99.21% and 98.77%, respectively. The similar surface area for PC1 and PC2 was 98.62% and 97.85%, respectively. The mean deviation value for PMMA1 and PC1 is the same (-0.14) and similarly, the mean deviation value for PMMA2 and PC2 is also the (-0.11). However, their standard deviations are different. The standard deviation of PMMA1 and PMMA2 are smaller than that of PC1 and PC2. This means that PC1 and PC2 have more variability than PMMA1 and PMMA2 respectively. PMMA2 has the smallest standard deviation: its data values are most concentrated around the mean. With the cube, the tolerances range of the castings from the PMMA patterns was smaller as compared to that of the PrimeCast® patterns. Most of features on the castings from the PrimeCast pattern has wider deviation range than that from the castings from PMMA pattern.

The chart in Figure **10** below represent the comparison in relative surface area of the castings from the two patterns. The relative surface area denoted in green of the casting from the PMMA pattern is 85 % and it is 17 % more than that of the casting from the PrimeCast® pattern. Red and blue is more on the casting from the PrimeCast® than in the casting from PMMA pattern. The overall difference in dimensional accuracy in the set tolerances range between the castings from the two patterns 0.5 %, and this is because almost all the surface area of the both castings were within this range.

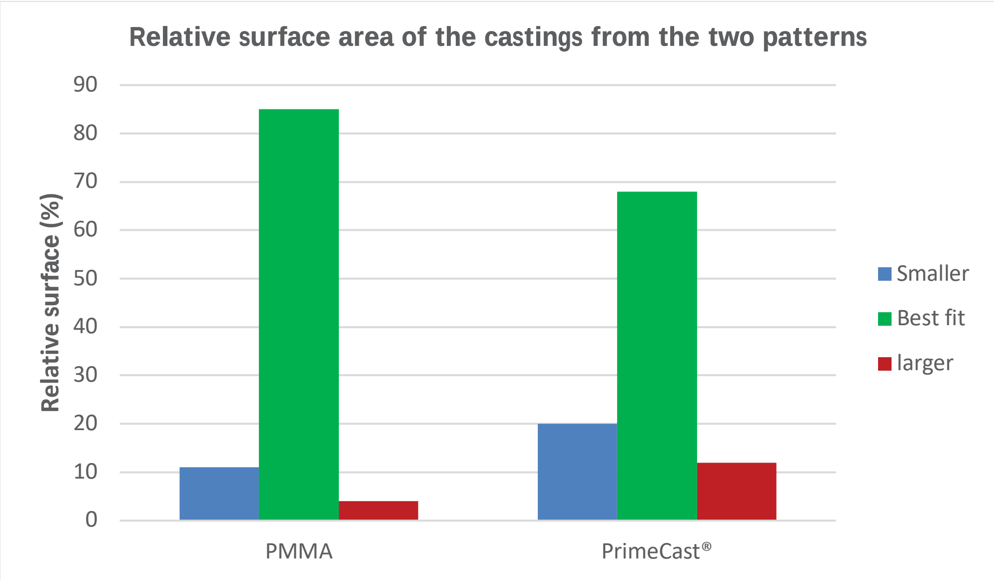

Figure 10: Comparison of relative surface area between the castings from the two patterns.

4. CONCLUSIONS

- The ability of PrimeCast® and PMMA materials to be used as sacrificial patterns for the investment casting process has been validated: Aluminium A356 was successfully cast from the two types of sacrificial patterns.
- Application of the RIC process has become the preferred choice for foundries that has adapted this technique, because of its suitability to manufacture complex parts with internal cavities, fast and cost effectively.
- The overall dimensional accuracy of castings from PMMA patterns show less differences in dimensional deviation compared to castings from PrimeCast® patterns.
- PrimeCast® patterns need more care during mould making and burnout processes compared to PMMA patterns. The need for removal of vents from castings produced from PrimeCast® patterns through grinding makes it easy to lose accuracy.
- Both AM materials burn out cleanly from the moulds and the final cast parts were acceptable.
- It is clear from the results obtained that for castings produced from PrimeCast® and PMMA patterns typical deviation of ±1.5 mm on average can be expected.
- Both PMMA and PrimeCast® patterns were impregnated with wax just after manufacturing. The sacrificial patterns produced from these two AM technologies are characterised by a significant porosity due to the manufacturing technique used therefore the impregnation is required. Impregnation can affect the dimensional accuracy of both patterns.

- Although there was visible difference in surface roughness between the castings from the two AM patterns, the surface roughness measurements were not performed because of the fact that impregnation also ensures low surface roughness.
- From the results it is not possible to tell which type of pattern produced the best castings; each pattern type had its advantages and limitations that will influence selection depending on the end user's application.

ACKNOWLEDGEMENTS

The active support and funding of the South African Department of Science and Technology through the CSIR for the Collaborative Program in Additive Manufacturing, Contract No.: CSIR-NLC-CPAM-15-MOA-CUT-01, are gratefully acknowledged.

The authors are grateful to Pierre Rossouw, Senior Researcher at CSIR, Material Science and Manufacturing, who is an expert in investment casting and led the casting trials.

The Centre for Rapid Prototyping and Manufacturing (CRPM) is also acknowledged for facilitating in redesigning of the PrimeCast® pattern.

REFERENCES

[1] Pattnaik, S., Karunakar, D.B. & Jha, P.K. 2012. Developments in investment casting process - A review', *Journal of Material Process Technology*, 212 (11), pp. 2332–2348.

[2] Ram Prasad. 2012. Progress in Investment Castings, *Science and Technology of Casting Processes'*, https://www.intechopen.com/books/science-and-technology-of-casting-processes/progress-in-investment-castings/ accessed 20-04-2018.

[3] Dimitrov, D., Hugo P.A. & Deez, B. 2008. Suitability of Layer Manufacturing Technologies for Rapid Pattern Making in Investment Casting of Light Metals', *Proceedings of the 9th Annual RAPDASA International Conference*, Central University of Technology, Free State, 13 – 15 November 2008, pp. 1–14.

[4] Cheah, C.M., Chua C.K., Lee, C.W., Feng, C. & Totong, K. 2005. Rapid prototyping and tooling techniques: a review of applications for rapid investment casting', *The International Journal of Advanced Manufacturing Technology*, 25 (1-2), pp. 308-320.

[5] Altaf, K., Rani, A.M.A., Woldemichael, E.D., Lemma1, A.T., Jian, C.Z. & Fiqri, M.H. 2016. Application of additive manufacturing / 3d printing technologies and investment casting for prototype development of Polycrystalline Diamond Compact (PDC) drill bit body', *Journal of Engineering and Applied Sciences,* 11 (10), pp 6514-6518.

[6] Anglada, E., Meléndez, A., Maestro, L., **&** Domiguez, I. 2013. Adjustment of Numerical Simulation Model to the Investment Casting Process', *Procedia Engineering,* 63, pp. 75-83.

[7] Prakash, S., Sharma, S. & Kumar, R. 2014. Microstructure and Mechanical Properties of A356 / SiC Composites Fabricated by Electromagnetic Stir Casting', *Procedia Materials Science,* 6, pp. 1524-1532.

[8] Goodridge, R.D. Tuck, C.J **&** Hague, R.J.M. 2012. Laser sintering of polyamides and other polymers,' *Progress on Material Science*, 57 (2), pp. 229–267.

[9] Wang, S. Miranda, A.G. **&** Shih, C. 2010. A Study of Investment Casting with Plastic Patterns,' *Material Manufacturing Process*, 25 (12), pp. 1482–1488.

[10] Marwah, O.M.F., Sharif, S., Sulaiman, S., Ibrahim, M., & E. J. Mohamad, E.J. 2014. Direct Investment Casting Numerical Study for ABS P400 FDM Materials', *Applied Mechanical Materials*, 660, pp. 99–103.

[11] Hsu, F., Jolly, M.R., & Campbell, J.A. 2009. Multiple-gate runner system for gravity casting', *Journal of materials processing technology*, pp 57.

[12] Mueller, T. 2017. A comparison of 3D printing technologies used to make investment casting patterns', https://www.slideshare.net/TomMueller1/a-comparison-of-3d-printing-technologies-used-to-make-investment-casting-patterns-part-3 accessed 28-06-2018.

[13] Bott, R. 2014. Dimensional accuracy of PMMA casting patterns produced by 3D printing after impregnation,' *Igarss 2014*, pp. 1–5.

[14] Polzin, C., Spath, S & Seitz, H. 2013. Characterization and evaluation of a PMMA-based 3D printing process,' *Rapid Prototyping Journal,* 19(1), pp. 37-43.

[15] Dotchev, K. and Soe, S. 2006. Rapid manufacturing of patterns for investment casting: Improvement of quality and success rate,' *Rapid Prototyping Journal*, 12 (3), pp. 156–164.

[16] Nkhasi, N., du Preez W. & van der Walt, J.G. 2008. Effectiveness of PrimeCast® and PMMA additive manufacturing Processes to produce patterns for investment casting', *Proceedings of the 18th Annual RAPDASA International Conference*, Durban ICC, 07 - 10 November 2017, pp. 62–64.

[17] Du Plessis, A. Gerhard, S. Guelpa A. 2016. The CT Scanner Facility at Stellenbosch University: An open access X-ray computed tomography laboratory', *Nuclear Instruments and Methods in Physics Research,* B (384), pp. 42-49.